Molecular Structure and Its Change: Hydrocarbons

Richard F. W. Bader,* Ting-Hua Tang,[1] Yoram Tal, and Friedrich W. Biegler-König

Contribution from the Department of Chemistry, McMaster University, Hamilton, Ontario, L8S 4M1 Canada. *Received June 1, 1981*

Abstract: The molecular structures of hydrocarbons as defined and determined by the topological properties of their charge distributions are presented and discussed. Among the structures determined are those for the protonated cyclopropanes. The edge-protonated structure, for example, possesses a four-membered ring formed by a bridging hydrogen atom. The possible mechanisms of structural change as determined by a mathematical theorem of structural stability are illustrated and discussed. The examples considered include hydrogen and methyl group migrations in carbocations, the formation of a cage structure in the propellane system by the rupture of the bridgehead bond, and the structural instability of the benzvalene molecule. This paper illustrates that the determination of the number and kind of critical points present in a molecular charge distribution enables one to assign unambiguously a chemical structure to the molecule and to determine whether or not it is structurally stable. If it is unstable, one may predict the possible ensuing structural changes.

I. Introduction

A theory of molecular structure, based upon the properties of the total charge distribution and their quantum mechanical consequences, has recently been developed. The theory demonstrates that the concepts of atoms and bonds may be rigorously defined and given physical expression in terms of the topological properties of the observable distribution of charge for a molecular system.[2] As a consequence of these definitions, one in turn obtains a definition of structure and a predictive theory of structural stability.[3,4] The theory is linked to quantum mechanics by demonstrating that the atoms so defined represent a class of open quantum subsystems with a unique set of variationally defined properties.[5-7]

In this paper we illustrate the theory through a study of the structures and the mechanisms of structural change for hydrocarbon molecules. The study considers cyclic and acyclic systems, both saturated and unsaturated, and also positively charged molecular ions. In the following paper,[8] the properties of the atoms and bonds which give rise to these structures are presented and discussed.

II. Calculations

The molecular charge distributions analyzed in this work are obtained from SCF calculations using the STO-3G basis set. Pople and his collaborators have established that STO-3G SCF calculations provide a theoretical model of the hydrocarbons at their equilibrium geometries which is in good agreement with experiment.[9-11] Individual carbon–carbon bond lengths are predicted to within 0.04–0.06 au (0.02–0.03 Å) of the experimental values. As important, observed trends in CH and CC bond lengths as well as in bond angles are well reproduced by this model. The small dipole moments found for certain of the hydrocarbons are, with few exceptions, also satisfactorily reproduced.

The principal aim of these papers is to use this theory of molecular structure to illustrate the role of the charge density in determining the regularities in the structures and properties observed for a family of molecules. The STO-3G theoretical model of the hydrocarbons is well suited for this purpose as the theoretical equilibrium geometries have been determined for a large number of hydrocarbons[9] and the molecular charge distributions may be economically calculated and analyzed. In addition, it is found that the observed trends in the properties of the charge distributions and the atomic charges for hydrocarbons determined by this basis set do not differ markedly from those obtained using fully optimized sets with polarizing functions. This is most likely a consequence of the small polarity of the bonds in hydrocarbon molecules.

III. Molecular Structure

Atoms and bonds are defined by the topological properties of the total charge distribution of a molecular system.[12] These definitions are made evident by the properties of the gradient vector field of the electronic charge density (Figure 1). The symbol $\rho(\mathbf{r},\mathbf{X})$ denotes the value of the electronic charge density at a point $\mathbf{r}$ in real space for a given geometrical arrangement of the nuclei $\mathbf{X}$, the vector $\mathbf{X}$ representing a given point in nuclear configuration space. The direction of the gradient vector $\nabla_r\rho(\mathbf{r},\mathbf{X}) \equiv \nabla\rho(\mathbf{r},\mathbf{X})$ is in the direction of maximum increase in $\rho(\mathbf{r},\mathbf{X})$. A gradient path is the integral curve of the differential equation

$$d\mathbf{r}(s)/ds = \nabla\rho(\mathbf{r}(s),\mathbf{X}) \tag{1}$$

for some initial value $\mathbf{r}(0) = \mathbf{r}_0$. Thus the points $\mathbf{r}(s)$ of the gradient path through $\mathbf{r}_0$ are given by

$$\mathbf{r}(s) = \mathbf{r}_0 + \int_0^s \nabla\rho(\mathbf{r}(t),\mathbf{X})\, dt \tag{2}$$

Every gradient path originates and terminates at a critical point in $\rho(\mathbf{r},\mathbf{X})$, a point where $\nabla\rho(\mathbf{r},\mathbf{X}) = 0$. A critical point is characterized by the eigenvalues of the matrix of second derivatives of $\rho(\mathbf{r}_c)$, $\nabla\nabla\rho(\mathbf{r}_c)$. Its rank equals the number of nonzero eigenvalues; its signature is the excess number of positive over negative eigenvalues. For critical points of rank 3, only four values of the signature are possible, yielding the critical points labeled by their rank and signature: (3,−3), (3,−1), (3,+1), and (3,+3). A (3,−3) critical point is a local maximum in $\rho(\mathbf{r})$, while a (3,+3) critical point is a local minimum. The remaining two critical points denote the presence of saddle points in the charge distribution and each defines a surface. The charge density is a maximum in the surface associated with a (3,−1) critical point at the position of the critical point. It is a minimum at the critical point with respect

(1) Department of Chemistry, Tianjin Teachers' College, Tianjin, People's Republic of China.
(2) R. F. W. Bader, S. G. Anderson, and A. J. Duke, *J. Am. Chem. Soc.*, **101**, 1389 (1979); R. F. W. Bader and P. M. Beddall, *J. Chem. Phys.*, **56**, 3320 (1972).
(3) R. F. W. Bader, T. T. Nguyen-Dang, and Y. Tal, *J. Chem. Phys.*, **70**, 4316 (1979).
(4) R. F. W. Bader, Y. Tal, S. G. Anderson, and T. T. Nguyen-Dang, *Isr. J. Chem.*, **19**, 8 (1980).
(5) S. Srebrenik and R. F. W. Bader, *J. Chem. Phys.*, **63**, 3945 (1975); S. Srebrenik, R. F. W. Bader, and T. T. Nguyen-Dang, *ibid.*, **68**, 3667 (1975); R. F. W. Bader, S. Srebrenik, and T. T. Nguyen-Dang, *ibid.*, **68**, 3680 (1978).
(6) R. F. W. Bader, *J. Chem. Phys.*, **73**, 2871 (1980).
(7) R. F. W. Bader and T. T. Nguyen-Dang, *Adv. Quantum Chem.*, **14**, 63 (1981).
(8) R. F. W. Bader, T. H. Tang, Y. Tal, and F. W. Biegler-König, *J. Am. Chem. Soc.*, following paper in this issue.
(9) J. A. Pople, "Electronic Structure Theory", Vol. III, H. F. Schaefer, Ed., Plenum, New York, 1977, pp 1–28.
(10) W. J. Hehre, in ref 9, pp 277–332.
(11) M. D. Newton, in ref 9, pp 223–276.

(12) We give a qualitative review of the definitions of the elements of molecule structure. This is sufficient for the understanding and the application of the theory. The reader who is interested in the rigorous mathematical expression of these definitions is referred to ref 3 and 4, or 24.

0002-7863/82/1504-0940$01.25/0

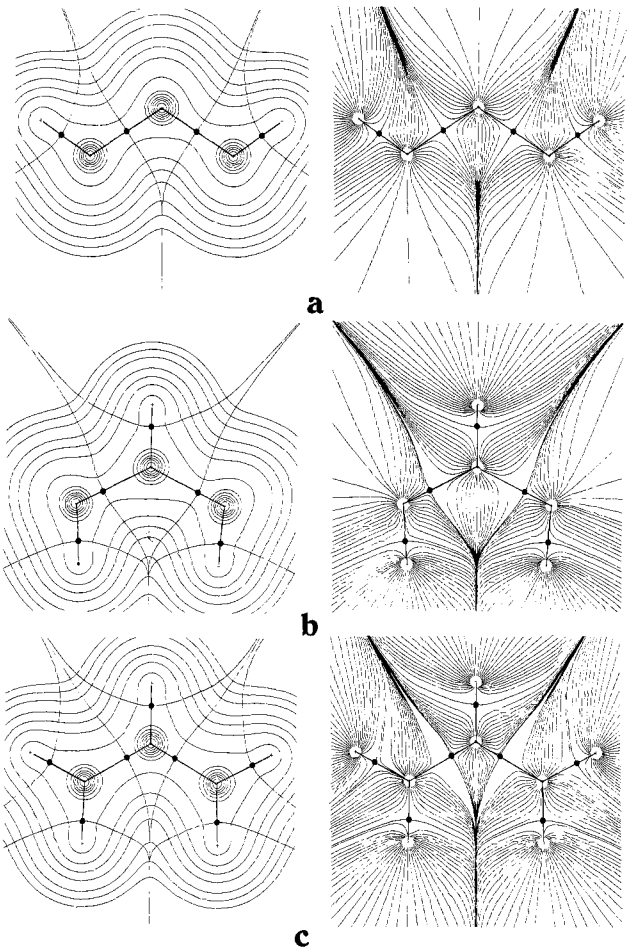

Figure 1. Contour plots of $\rho(\mathbf{r})$ and displays of the gradient vector fields of $\rho(\mathbf{r})$ for (a) propane, $CH_3CH_2CH_3$; (b) 2-propyl cation, CH_3CHCH_3; (c) allyl cation, CH_2CHCH_2. In each case the plane illustrated contains the three carbon nuclei. In the displays of the gradient vector fields, each line represents a trajectory of $\nabla\rho(\mathbf{r})$. The set of trajectories which terminate at a given nucleus or attractor defines the basin of that attractor. The pair of trajectories which, in this plane, terminate at each (3,−1) or bond critical point (denoted by a solid circle) mark the intersection of an interatomic surface with the plane of the figure. The trajectories which originate at the bond critical points and define the bond paths are shown in heavy line. The trajectories associated with the bond critical points are superimposed on the contour maps of $\rho(\mathbf{r})$. These trajectories define the boundaries of the atoms and the molecular graph. The values of the contours increase from the outermost one inward in steps of 2×10^n, 4×10^n, and 8×10^n with n beginning at −3 and increasing in steps of unity. The projected positions of out-of-plane nuclei are indicated by open crosses.

to motion away from the critical point in a direction normal to the surface. The properties of a (3,+1) critical point are just the reverse of those for a (3,−1) critical point.

The local maxima in $\rho(\mathbf{r},\mathbf{X})$ occur at the positions of the nuclei.[13] Each nucleus, therefore, acts as a point attractor in the associated gradient vector field $\nabla\rho(\mathbf{r},\mathbf{X})$. That is, all the gradient paths in the vicinity of a given nucleus terminate at that nucleus. The region of space traversed by the gradient paths which terminate at a given attractor is the *basin* of that attractor. Since the nuclei are the only attractors of the field $\nabla\rho(\mathbf{r},\mathbf{X})$, the total space of a molecular system is partitioned into disjoint regions, the basins, each of which contains one and only one point attractor or nucleus (Figure 1). *An atom, free or bound, is defined as the union of an attractor and its associated basin.* This definition results in a partitioning of the real space of a molecular system into a collection of nonoverlapping atomic regions.

There is a saddle point in $\rho(\mathbf{r},\mathbf{X})$ between each pair of neighboring atomic basins. These are (3,−1) or bond critical points and their positions are denoted by a solid circle. In the symmetry planes shown in Figure 1, two gradient paths terminate at each such critical point and define the common boundary of two neighboring atomic basins. The set of all gradient paths which terminate at a bond critical point between two atoms A and B defines the *interatomic surface* S_{AB} in three-dimensional space. The atomic surface S_A of an atom A is defined as the boundary of its basin. Hence $S_A \supset U_B S_{AB}$. Clearly the space occupied by an atom is defined by the union of a given attractor and its associated basin, or by its atomic surface. An atomic surface $S(\mathbf{r})$ possesses the particular property of exhibiting a zero flux in the gradient vectors of $\rho(\mathbf{r},\mathbf{X})$ at every point of the surface,

$$\nabla\rho(\mathbf{r},\mathbf{X})\cdot\mathbf{n}(\mathbf{r}) = 0 \qquad \forall \mathbf{r} \in S(\mathbf{r}) \tag{3}$$

where $\mathbf{n}(\mathbf{r})$ is a unit vector normal to the surface at $\mathbf{r}$. It is this property of zero flux which imparts to the atom its particular quantum mechanical properties.[6,7] The union of two or more adjacent atoms is again a connected region bounded by a zero flux surface. Thus one may define and examine the properties of chemically significant functional groups, such as $-CH_3$ and $-CH_2-$ in the present work.

A bond saddle point serves as the origin for two gradient paths, each of which terminates at one of the neighboring nuclei. Together they define a line through space linking neighboring nuclei along which the charge density is a maximum with respect to a lateral displacement. Such a line is called a *bond path*.[14,15] The network of such bond paths for a given nuclear configuration $\mathbf{X}$ defines a *molecular graph*. A *molecular structure* is then defined as an equivalence class of molecular graphs. That is, the same number of bond paths link the same nuclei in each molecular graph belonging to a given molecular structure. In general, it is found that one may associate a given molecular structure with an open neighborhood of an energetically stable geometry of a system. Thus, the network of "chemical bonds" (a given chemical structure) is invariant to the vibrations and internal rotations of an energetically stable system.

Figure 2 illustrates the molecular graphs for the hydrocarbon molecules studied here, at their equilibrium geometries. Each diagram is a computer-generated projection of the molecular graph determined by the theoretical charge distribution. The positions of the (3,−1) or bond critical points are indicated by solid circles. The bond-path networks predicted by the molecular graphs coincide with the usual structures assigned to these molecules. A bonded ring of atoms, such as found in C_3H_6 (F) or C_4H_8 (G), denotes the presence of a (3,+1) critical point whose surface defines the surface of the ring. The charge density is a minimum in the ring surface at this critical point. The charge distribution of a cage structure, for example, C_4H_4 (H) or C_5H_8 (V), contains a (3,+3) critical point in the interior of the bonded cage of atoms. The charge density within the cage attains its minimum value at such a critical point. Each cage is bounded by some number of ring surfaces, four in C_4H_4 and three in C_5H_8. In C_4H_4 the (3,+1) or ring critical points are found to be outwardly displaced from the geometrical perimeters of the C_3 rings forming the faces of the cage. Hence the ring surfaces, as well as the bond paths, are

(13) This is a well-established observation. For example, in the approximately 70 molecular charge distributions determined in this research on the hydrocarbons, only the acetylene molecule and its methyl derivative exhibited a local maximum in $\rho(\mathbf{r})$ at a position other than at the nuclei. At the STO-3G level of approximation, the charge distributions for these two molecules exhibit a local maximum on the axis between the acetylenic carbons. The values of the charge density at these exceptional maxima exceed those of neighboring minima on the same axis by only 0.003 au, or approximately 1% of the value of $\rho(\mathbf{r})$ at these maxima. In better approximations to the charge distributions for acetylenic molecules, these spurious maxima are no longer present. As previously discussed,[2,4] the maximum in ρ at a nuclear position is not a true critical point as $\nabla\rho$ is discontinuous there because of the cusp condition on ψ. However, there always exists a function homeomorphic to $\rho(\mathbf{r})$, which coincides with ρ almost everywhere, and for which the nuclei are (3,−3) critical points. In this sense, the nuclear positions in $\rho(\mathbf{r})$ behave topologically as do (3,−3) critical points.

(14) R. F. W. Bader, *MTP Int. Rev. Sci. Phys. Chem., Ser. Two*, **1**, 43 (1975).

(15) G. R. Runtz, R. F. W. Bader, and R. R. Messer, *Can. J. Chem.*, **55**, 3040 (1977).

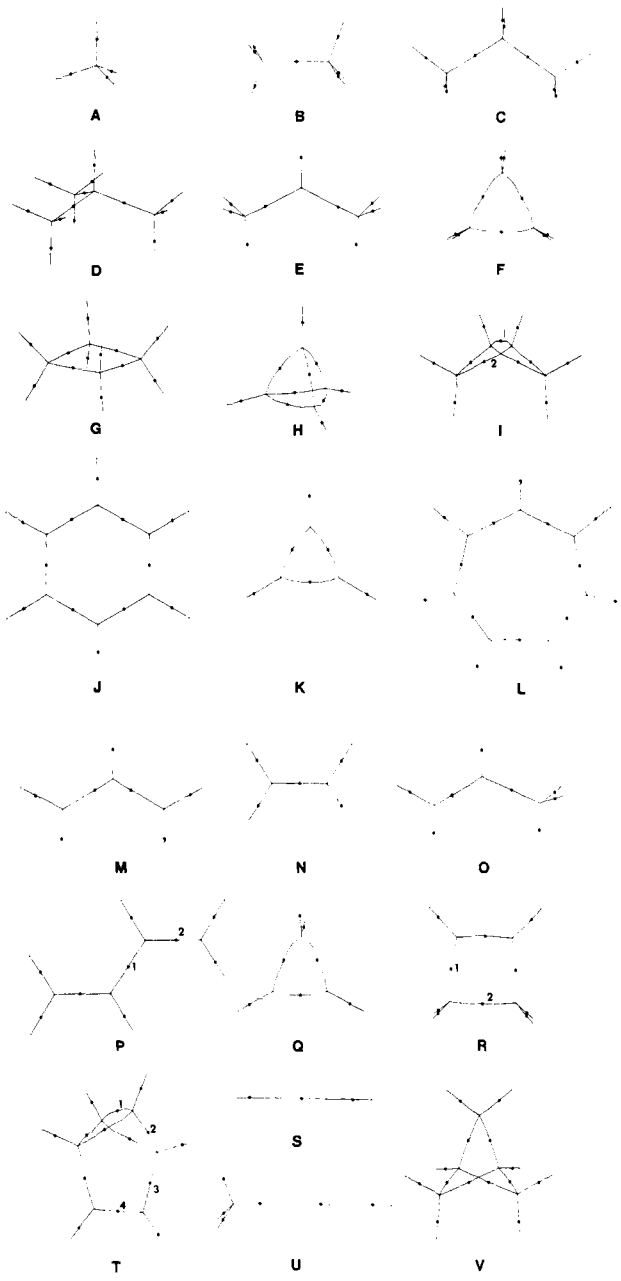

Figure 2. Computer generated projections of the molecular graphs for hydrocarbon molecules in their equilibrium geometries as determined by the topological properties of their charge distributions: (A) methane, (B) ethane, (C) propane, (D) isobutane, (E) 2-propyl cation, (F) cyclopropane, (G) cyclobutane, (H) tetrahedrane, (I) bicyclo[1.1.0]butane, (J) benzene, (K) cyclopropenium cation, (L) tropylium cation, (M) allyl cation, (N) ethylene, (O) propene, (P) 1,3-*trans*-butadiene, (Q) cyclopropene, (R) cyclobutene, (S) acetylene, (T) benzvalene, (U) methylacetylene, (V) bicyclo[1.1.1]pentane.

outwardly curved. In C_5H_8 (V) the ring surfaces are strongly curved toward the interior of the cage. The number and kind of each critical point in a molecular graph satisfy the relation

$$n - b + r - c = 1 \qquad (4)$$

where n equals the number of nuclei (or (3,−3) critical points), b the number of bonds (or (3,−1) critical points), r the number of rings (or (3,+1) critical points), and c the number of cages (or (3,+3) critical points).[16]

In those structures which are considered to be strained, for example, bicyclo[1.1.0]butane (I), the bond paths are outwardly curved from the geometrical perimeter of the ring or cage. This topological evidence of strain is given quantitative expression through the definition of a bond energy in the following paper.[8] While single, double, and triple bonds are topologically indistinguishable, they are differentiated one from the other in terms of the properties of $\rho(\mathbf{r})$ at the corresponding bond critical points. These properties serve to define a bond order.[8] A bond critical point between inequivalent carbon atoms is not equidistant from the two nuclei (see E and M, for example). The resulting increase or decrease in the bonded radius generally implies a corresponding increase or decrease in the average number of electrons associated with the atom.[8] A significant amount of chemical information is summarized by a molecular graph and the properties of $\rho(\mathbf{r})$ at the bond critical points which define it.

The assignment of a network of bonds to an equilibrium structure on the basis of theories of valence is in general found to be consistent with the interpretation of vibrational spectra in terms of valence force potential fields, with the observation of characteristic internuclear separations (i.e., bond lengths), and with thermochemical data on energies of formation and reaction. The assumption of the existence of a network of bonds thus results from a synthesis of information obtained from a wide range of physical observations. What is remarkable is that these many avenues of approach to the assignment of bonds may be viewed as attempts to determine which nuclei in a molecule are linked by lines along which the charge density is a maximum—to determine the network of bond paths.

IV. Changes in Structure

The definition of structure as an equivalence class of molecular graphs leads to a partitioning of the nuclear configuration space of a chemical system into a finite number of structural regions, each region denoting a possible structure of the system. The boundary of a structural region denotes the configurations of transitional or unstable structures which separate a stable structure from neighboring ones. This structural information constitutes a *structure diagram*, a diagram which determines all possible structures and all mechanisms of structural change for a given chemical system. A given structure belongs to an open region of nuclear configuration space while the boundaries (hypersurfaces) separating two structural regions are closed regions, and a change in structure is therefore an abrupt or discontinuous process.

This definition of molecular structure coincides with the original intent of the notion of structure in chemistry—that it be a generic property of a system. Structure implied a particular network of chemical bonds which was presumed to exist over a range of nuclear displacements until some geometrical parameter attained a critical value at which point bonds were assumed to be broken and/or formed to yield a new structure. A change in structure is exemplified by the succession of molecular graphs shown in Figure 3 for the migration of a proton in the $C_2H_5^+$ system, that is, for the reaction

$$H\text{–}CH_2\text{–}CH_2^+ \rightarrow CH_2^+\text{–}CH_2\text{–}H \qquad (I)$$

At the STO-3G level of approximation, the geometries of the open structures a or e (Figure 3) are the equilibrium geometries for this ion and the structure c is for the geometry of the transition state, 11.0 kcal/mol above the energy of the equilibrium structure.[10] As a proton on the methyl group is displaced from its equilibrium position in Figure 3a to yield the new geometry in 3b, it remains linked to the same carbon atom by a bond path and the molecular graph remains unchanged. Thus the structure associated with the equilibrium geometry persists for motion along the reaction path. However, when the energy attains its maximum value at the geometry of the transition state, there is a sudden change in structure as the bond path from the proton switches from carbon to the CC bond critical point (Figure 3c). This structure is unstable; it exists for a single geometry along the reaction path. It is transitional between the structures of the reactant and product molecules and a further infinitesimal motion of the proton causes the bond path to switch to the second carbon atom to yield the structure of the product molecule. This mechanism, which proceeds by a switching of attractors, is also found for the isomerization reactions of HCN and CH_3CN to their

(16) K. Collard and G. G. Hall, *Int. J. Quantum Chem.*, **12**, 623 (1977).

corresponding isocyanides.[17] The energy profiles for these reaction paths also exhibit a single energy maximum, and the switching of the H or CH_3 bond path from C to N is again found to occur at (or computationally in the immediate vicinity of) the corresponding transition state.

The unstable structure in Figure 3c is termed a conflict structure. The point in nuclear configuration space corresponding to this structure is called a catastrophe point. The set of catastrophe points comprises the hypersurfaces which partition nuclear configuration space into structural regions to yield a structure diagram. A schematic representation of the structure diagram for an ABC system is shown in Figure 4. Each of the letters may denote a single atom or a grouping of atoms. This diagram predicts a second possible mechanism for a reaction of the type shown in (I) for the conversion of ABC to BCA. This second mechanism involves the formation of an intermediate ring structure. It is illustrated by the migration of a CH_3 group in $C_3H_7^+$,

$$CH_3\text{–}CH_2\text{–}CH_2^+ \rightarrow {}^+CH_2\text{–}CH_2\text{–}CH_3 \qquad \text{(II)}$$

as illustrated by the second set of molecular graphs shown in Figure 3. The geometry indicated by the molecular graph in Figure 3f is the second most stable equilibrium geometry of the $C_3H_7^+$ ion.[10] The molecular graph associated with this minimum energy geometry persists for motion of the CH_3 group across the $H_2C\text{–}CH_2$ bond until the geometry indicated in Figure 3g is attained. At this geometry an unstable or degenerate critical point, one of rank two, is formed within the charge distribution. Associated with this critical point is a pair of trajectories which link the methyl group with the second CH_2 group. This structure is unstable and it lies on the surface separating the open structural region from the ring structural region on the structure diagram. Further motion of the methyl group results in the bifurcation of this unstable critical point into two nondegenerate or stable critical points, a (3,–1) or bond critical point connecting the methyl group with the second CH_2 group and a (3,+1) or ring critical point, and the ring structure is obtained (Figure 3h). Continued motion of CH_3 across the $H_2C\text{–}CH_2$ bond causes the ring critical point to migrate toward the bond critical point which formed the original bond path to the CH_3 group. When these two critical points coalesce, the system is at a second bifurcation catastrophe point, and at the boundary between the ring region and the structural region of the product. At this point, the original bond path is broken and the system point enters the structural region of the product molecule (Figure 3j).

In the example of the conflict mechanism, the geometry of the topologically unstable structure which signals the change in structure coincides with the energetically unstable geometry of the transition state. If this coincidence in the geometries of topologically and energetically unstable structures is a general property of molecular systems,[17] then one would expect the energy profile for the mechanism involving the formation of a structurally stable ring intermediate to exhibit two maxima, the two transition states corresponding to the two bifurcation catastrophe points which denote the formation and subsequent destruction of the ring structure. This is not found to be the case at the STO-3G level where instead the energy profile is predicted to exhibit a single maximum.[18] However, it is clear from the narrow nature of the ring in Figure 3h that the reaction path traverses the ring region of the structure diagram Figure 4, close to the apex where the bifurcation catastrophe set merges with the set of conflict structures. Indeed, it is found that a small outward displacement of the CH_3 group causes the structure shown in Figure 3h to change into an unstable conflict structure. This change in structure occurs for the configuration at which the ring critical point and the critical points of the bonds linking the methyl group coalesce. The values of $\rho(r)$ at the bond and ring critical points of the ring structure are almost identical, being 0.1221 and 0.1220 au, respectively. Thus the minimum in the energy path corresponding to the ring structure is expected to be shallow, and at the STO-3G level of approximation it is not found. Indeed, the energy barrier for this reaction is itself predicted to be only 3 kcal/mol at the STO-3G level of approximation.[18] The changes in the atomic charges and bond orders which occur in reactions I and II are discussed in the following paper.[8]

The structures of other higher energy equilibrium geometries of $C_3H_7^+$ are also shown in Figure 3. At the STO-3G and 4-31G levels of approximation, the most stable geometry of this cation is the 2-propyl cation shown in Figure 2E. The next most stable ($\sim$20 kcal/mol above the 2-propyl cation) are the 1-propyl cation (Figure 3f) and the corner-protonated cyclopropanes (Figure 3h).[18] The edge-protonated structure of cyclopropane (Figure 3k) has an energy 27 kcal/mol above that of the 2-propyl cation. Note that this structure consists of a four-membered ring with no bond path linking the carbons joined by the bridging hydrogen. The least stable geometry is found for the face-protonated form of cyclopropane (Figure 3l). In this structure the proton is linked by a bond path to the (3,+1) or ring critical point. This is another example of an unstable conflict structure. Any motion of the proton away from the symmetry axis results in a change in structure to one wherein the proton is bonded to a carbon atom as illustrated in Figure 3m.

The structure shown in Figure 3n is for the equilibrium geometry of the CH_5^+ cation. It corresponds to a methyl group bonded to one proton of H_2. As discussed in the following paper,[8] the methyl group bears a net charge of +0.55 e and the H_2 group a charge of +0.45 e. This particular configuration lies close to a conflict catastrophe point, and hence the bond from carbon switches from one proton of H_2 to the other (Figure 3o). Since the energy hypersurface is relatively flat in the neighborhood of the equilibrium geometry with respect to internal motions of the H_2 group[19,20] (the structures in 3n and 3o differ by $\sim$1 kcal/mol), the bond from carbon is constantly switching between the protons during the course of the molecule's internal motions.

An interesting change in structure is exhibited by the [1.1.1]propellane molecule, C_5H_6. The characteristic set of critical points (n, b, r, c) exhibited by the equilibrium charge distribution of this molecule is (11, 13, 3, 0) showing that its structure consists of three fused three-membered rings (Figure 5a). With little increase in energy, this structure is transformed into a cage structure by breaking the bond between the bridgehead carbon atoms. That this bond is long and weak in the equilibrium structure may be seen by comparing the charge distribution for one of three-membered rings with that for the cyclopropane molecule C_3H_6 (Figure 5).[21] The CC bond lengths in C_3H_6 are

(17) Y. Tal, R. F. W. Bader, T. T. Nguyen-Dang, M. Ojha, and S. G. Anderson, *J. Chem. Phys.*, **74**, 5162 (1981).

(18) L. Radom, J. A. Pople, V. Buss, and P. v. R. Schleyer, *J. Am. Chem. Soc.*, **94**, 311 (1972).

(19) W. A. Lathan, W. J. Hehre, and J. A. Pople, *Tetrahedron Lett.*, **31**, 2699 (1970).

(20) V. Dyczmons and W. Kutzelnigg, *Theor. Chim. Acta*, **33**, 239 (1974).

(21) Newton[11] and Newton and Schulman[22] have argued against the presence of a bond between the bridgehead carbons in propellane. They show a plot of $\rho(r)$ for this molecule calculated using the 4-31G basis set for the same plane as that given in this paper in Figure 5. Their plot does not include the contour which passes through the bond critical point of the bridgehead carbons. Thus the charge density *appears* to decrease monotonically from the apical carbon nucleus, forming a valley between the bridgehead atoms. We have calculated $\rho(r)$ for this molecule using both the STO-3G and 4-31G basis sets. The charge densities displayed in Figure 5 are from 4-31G calculations, and the contours displayed, with the exception of the one of value 0.161 au, are those shown by Newton and Schulman. A determination of the critical points shows that there is a bond critical point between the bridgehead carbons in both cases and, correspondingly, three near neighboring (3,+1) ring critical points. Thus $\rho(r)$ does not decrease monotonically along a C_2 axis from an apical carbon. Its profile along this axis exhibits a minimum at a (3,+1) critical point and a small maximum at the (3,–1) bridgehead bond critical point. An increase in the separation of the bridgehead carbon atoms causes this maximum and minimum in ρ to coalesce. The profile of ρ along this axis then exhibits a singularity; i.e., both $\partial\rho/\partial x$ and $\partial^2\rho/\partial x^2$ vanish. For further extension, this degenerate critical point vanishes, the bond is broken, and ρ does decrease monotonically along the axis. Critical points in close proximity and with similar $\rho(r)$ values may be easily missed in a contour plot of $\rho(r)$. The use of a program which searches for every critical point in a molecular charge distribution and determines its rank and signature overcomes this problem.

(22) M. D. Newton and J. M. Schulman, *J. Am. Chem. Soc.*, **94**, 773 (1972).

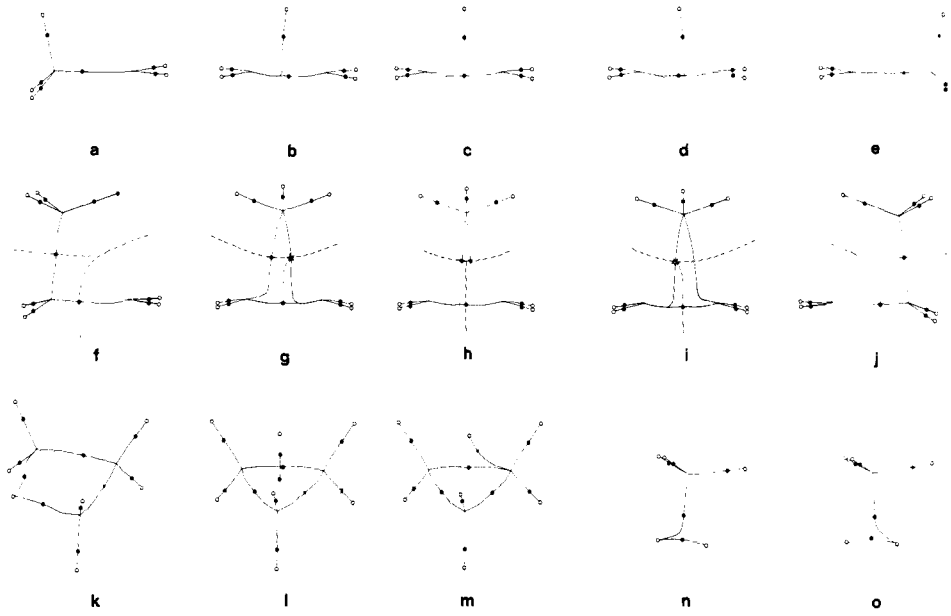

Figure 3. The molecular graphs a → e illustrate the migration of a proton in the $CH_3CH_2^+$ system (reaction I). The open circles denote the positions of the protons; the solid circles denote the bond critical points. Graphs a and b belong to the same structural region. The transition state, graph c, is a conflict structure, the unstable structure transitional between reactant and product structures. Molecular graphs f–j illustrate the migration of a methyl group in the $CH_3CH_2CH_2^+$ system, reaction II. The CC interatomic surfaces are denoted by dashed lines. Structures g and i are unstable. Their geometries correspond to bifurcation catastrophe points which lie on two of the surfaces bounding the ring structural regions (Figure 4). The unstable or degenerate critical point in these structures is denoted by a star. Moving from left to right, the star critical point suddenly appears at the geometry g and subsequently for further motion bifurcates into a bond and a ring critical point. The ring critical point migrates in a direction opposite to that of the methyl group and at i it coalesces with the initial CCH_3 bond critical point to create a star critical point and a second unstable structure. Note that in graphs a and f the CC bond critical points linking the CH_2 fragments are very unsymmetrically placed. In both molecules, the C of CH_2 bears a net negative charge.[8] In graphs c and h, the H_2C–CH_2 bond has a bond order of 1.5.[8] Figure 3k is an edge-protonated cyclopropane, a four-membered ring with a bridging H atom. Figure 3l is face-protonated cyclopropane, an unstable structure. The ring critical point is denoted by a solid square. Figure 3m is a stable structure obtained from l by a motion of the H atom away from the symmetry axis. Figures n and o are two structures for CH_5^+ which are close in energy and separated by a conflict structure wherein the bond path from C terminates at the bond critical point of the H_2 fragment.

2.84 au, and the value of the charge density at a (3,−1) CC bond critical point is 0.222 au, typical of CC single bonds at the 4-31G level of approximation. In C_5H_6, the bridgehead bond length is 3.02 au. This increased separation over that for C_3H_6 has two effects on the charge distribution: (a) the value of $\rho(r)$ at the CC bond critical point is greatly reduced, to 0.161 au; (b) the (3,+1) ring critical point is in the immediate proximity of the CC bond critical point, and the value of the charge density at this point is of almost equal value, 0.157 au. This proximity of the (3,+1) ring and (3,−1) bond critical points portends the instability of this system. An increase in the separation between the bridgehead carbon atoms results in the coalescence of the (3,−1) bond critical point with all three of the (3,+1) ring critical points to create a singularity in $\rho(\mathbf{r})$ and an unstable structure (Figure 5b). As illustrated in Figure 5c, a further increase in the bridgehead separation causes this singularity to bifurcate, to yield the elements of a cage structure, i.e., a (3,+3) critical point and three (3,+1) critical points. This cage structure with the characteristic set (11, 12, 3, 1) is bounded by three ring surfaces. Each of the ring surfaces contains two apical carbon nuclei, as well as the two bridgehead carbons, and hence is characterized by substantial curvatures. In effect the extension of the CC bridgehead bond causes each of the three ring critical points to move along a C_2 symmetry axis through the critical point of the bridgehead bond, at which point a change in structure occurs, to a point lying outside of the original three-membered ring it defined. The result is that the three planar three-membered rings of the original structure are transformed into three inwardly curved four-membered rings of the cage structure.

The instabilities of the conflict structures discussed above are predicted by a theorem of structural stability stated by Palis and Smale.[23] This theorem demonstrates that the conflict structures such as those found in HCN, $C_2H_5^+$, and CH_5^+, wherein a bond path (the unstable manifold) of one (3,−1) critical point is contained in the interatomic surface (the stable manifold) of a second (3,−1) critical point, are structurally unstable. The same theorem predicts that the coincidence of the bond path of a (3,−1) critical point with the unique axis (the stable manifold) of a (3,+1) ring critical point, as found for face-protonated cyclopropane, Figure 3l, is also unstable. The theorem shows the existence of a third possible type of unstable conflict structure. In this case the axis of one ring critical point is contained in the surface of another ring critical point. The benzvalene molecule (Figure 2T), an isomer of benzene, exemplifies this type of structural instability. The characteristic set for this molecule is (12, 14, 3, 0). It is not a cage structure. The vector field of $\rho(\mathbf{r})$ for this molecule is displayed in Figure 6 for a plane which bisects the bond between the bridgehead carbon atoms. The unique axes of the two three-membered rings (whose surfaces are perpendicular to the plane shown in the figure) are contained in the surface of the ring formed by four carbon atoms and the (3,−1) critical point of the bridgehead bond. This structure is unstable with respect to a change in the conformation of the pseudo-five-membered ring. Any motion which destroys the plane of symmetry illustrated in the diagram causes the pseudo-ring to change into a true five-membered ring, one composed of the four carbon atoms shown in the figure and one of the bridgehead carbons. The particular intersections of stable and unstable manifolds of critical points which yield the three possible kinds of unstable conflict structures described above are termed nontransversal intersections.[23] A detailed discussion of the theorem of Palis and Smale as applied to the structural changes in molecular systems is given elsewhere.[24]

A determination of the number and kind of critical points present in a molecular charge distribution enables one to unambiguously assign a structure to the molecule. According to the

(23) J. Palis and S. Smale, *Global Anal. Proc. Pure Math., AMS Symp. Pure Math.*, **14**, 223 (1970).

(24) R. F. W. Bader, T. T. Nguyen-Dang, and Y. Tal, *Rep. Prog. Phys.*, **44**, 893 (1981).

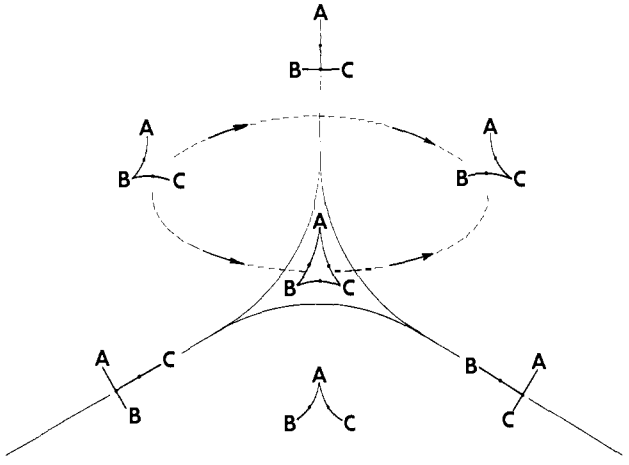

Figure 4. A two-dimensional cross section of the structure diagram for an ABC system. The solid lines, denoting the catastrophe set, partition the three-dimensional nuclear configuration space into its structural regions. The coordinates in this plane are two of the three internal displacement coordinates of an ABC system. The structure associated with each region is indicated by a representative molecular graph. The upper dashed line indicates a reaction path for the conflict mechanism found for reaction I, and the lower one, a reaction path for the bifurcation mechanism found for reaction II.

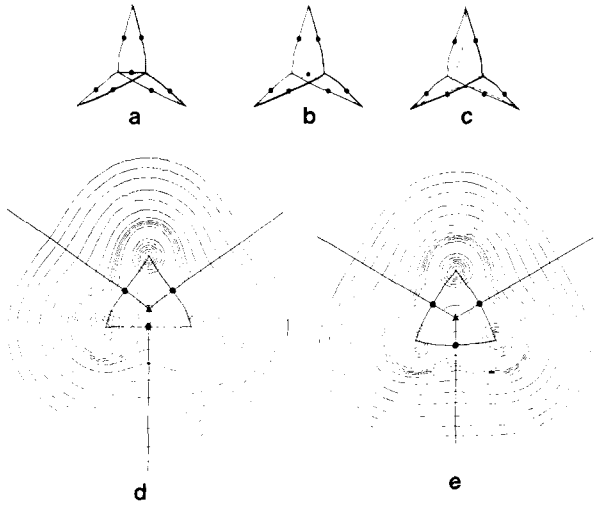

Figure 5. Molecular graphs, a–c, of three geometries of the [1.1.1]propellane system, C_5H_6. The two CH bond paths which terminate at each apical carbon are not shown. The dashed lines represent profiles of the ring surfaces: (a) the equilibrium geometry and (b) the geometry of the bifurcation catastrophe point. At this geometry the three ring critical points merge with the bridgehead bond critical point to yield the singularity in $\rho(r)$ denoted by a solid square. This structure is unstable. If the CC bridgehead separation is decreased from this value, one regains the structure shown in (a). If this distance is increased, the CC bond path vanishes and one obtains the cage structure shown in (c). Figures d and e are respectively contour plots of $\rho(r)$ for the plane of one three-membered ring in C_5H_6 and, for comparison, the ring of cyclopropane. The contour value are those used in ref 11 and 21 for C_5H_6 with the additional contour corresponding to the value of $\rho(r)$ at the bond critical point of the bridgehead carbons, 0.161 au. This contour is bracketed by contours of values 0.150 and 0.175 au. The innermost contour encircling all three carbons is 0.200 au. The shape of this latter contour is to be contrasted between (d) and (e). A (3,+1) ring critical point is denoted by a solid triangle, at which point $\rho(\mathbf{r})$ attains its *minimum* value in the ring surface, 0.157 au in C_5H_6 and 0.175 au in C_3H_6. Note the proximity of the ring critical point to the CC bridgehead bond critical point in (d). The same behavior is observed in C_3H_6 if one of the CC separations is increased.

theorem of Palis and Smale,[23] if all of the critical points are nondegenerate, i.e., are of rank three, and there are no nontransversal intersections between the manifolds of the (3,+1) and/or (3,−1) critical points, the structure is stable and it will persist over some range of neighboring geometries. A degenerate critical point is mathematically unstable in the sense that, under any perturbation of the charge density caused by a nuclear displacement, the critical point either vanishes or bifurcates into a number of nondegenerate or stable critical points. Correspondingly, a structure containing such a critical point is unstable and the associated nuclear configuration is a bifurcation catastrophe point. Examples are the formation and destruction of a ring structure (Figure 3) through the formation of a degenerate critical point which bifurcates into a (3,+1) and a (3,−1) critical point, and the formation of the cage structure in Figure 5 via a degenerate critical point formed by the coalescence of one (3,−1) and three (3,+1) critical points which bifurcates into one (3,+3) and three (3,+1) critical points. A structure is also unstable if it exhibits one of the three possible nontransversal intersections which, as discussed above, yield unstable structures corresponding to conflict catastrophe points in nuclear configuration space.

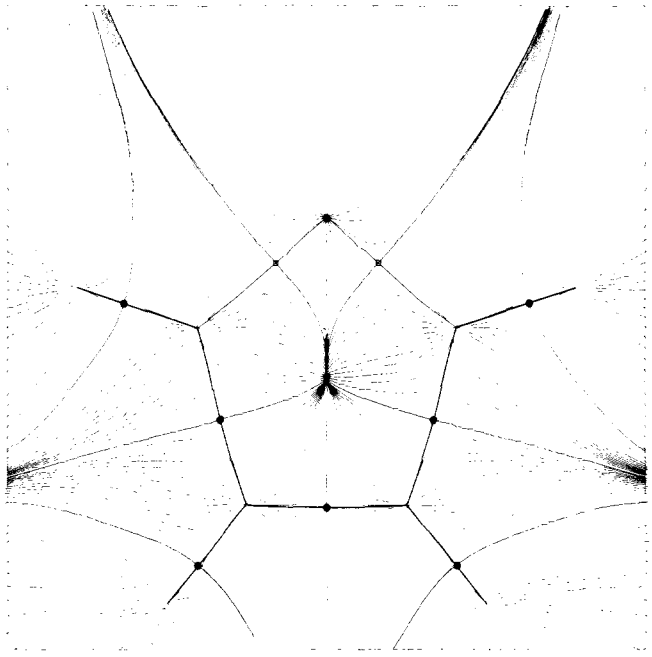

Figure 6. Display of the gradient vector field of $\rho(r)$ in benzvalene, C_6H_6 (Figure 2T), in the symmetry plane containing four carbon atoms (each bonded to a hydrogen) and the bond critical point of the CC bridgehead bond. The ring critical points of the two three-membered rings whose surfaces are perpendicular to this plane are denoted by open squares. The axes of these two ring critical points are contained in the surface of the unstable pseudo-ring formed by the four carbons and the bridgehead bond critical point.

The study of the hydrocarbons has yielded further examples of the equivalence between a molecular graph, as determined by the topological properties of a charge distribution for an equilibrium geometry, and the assignment of the network of chemical bonds to yield a molecular structure. The study has also yielded examples of the possible types of stable structures (open networks, rings, and cages) and of the essential generic property of structure, that it persist over some open neighborhood of an equilibrium geometry. It has also provided examples of the mechanisms of structural change, all of which proceed through the formation of an unstable structure associated with either a bifurcation or conflict catastrophe point in nuclear configuration space.

Acknowledgment is made to the donors of the Petroleum Research Fund, administered by the American Chemical Society, for partial support of this research.

Registry No. A, 74-82-8; B, 74-84-0; C, 74-98-6; D, 75-28-5; E, 19252-53-0; F, 75-19-4; G, 287-23-0; H, 157-39-1; I, 157-33-5; J, 71-43-2; K, 26810-74-2; L, 26811-28-9; M, 1724-44-3; N, 74-85-1; O, 115-07-1; P, 106-99-0; Q, 2781-85-3; R, 822-35-5; S, 74-86-2; T, 659-85-8; U, 74-99-7; V, 311-75-1; [1.1.1]propellane, 35634-10-7; $CH_3CH_2^+$, 14936-94-8; $CH_3CH_2CH_2^+$, 19252-52-9.